Investigating Fused Silica Bending Strength and Damping Characteristics on Resonators Fabricated through Femtosecond Laser-Assisted Wet Etching: An Experimental Analysis

Loïc Amez-Droz[1,2], Matéo Tunon de Lara[2,3], Anthony Amorosi[1,4], Pierre Lambert[2], Christophe Caucheteur[3] and Christophe Collette[1,4]

***Abstract*— Fused silica, renowned for its optical transparency and exceptional mechanical properties, including a high elastic range, challenges traditional material selection for compliant mechanisms. Leveraging femtosecond laser-assisted wet etching to machine three-dimensional fused silica structures, this study investigates the elastic range and damping characteristics of micro-scale monolithic bending specimens. Experimental results offer insights into the fused silica material application range for precision sensors and resonator design. Bending stress estimations are reported between 1.1 GPa and 2.7 GPa and a quality factor $Q = 1.85 \times 10^5$ at a pressure of 2×10^{-3} mbar.**

I. INTRODUCTION

Fused silica is best known for its use in optics due to its transparent properties. This material has also a very high elastic range that can be defined as its elastic limit (> 1GPa) to Young modulus (72 GPa) ratio. Being larger than Steel, Titanium or Copper-Beryllium. With its elastic modulus being in the same range as those materials, fused silica can replace them for the design of compliant mechanisms. Being a brittle material, its use was limited due to the machining complexity in the past. Nowadays, 3D structure manufacturing is possible by femtosecond laser-assisted wet etching [1]. Various compliant mechanisms have been obtained using this technique [2]–[4]. Thanks to its bio-compatibility, fused silica is also used to design surgical tools [5], [6]. We have demonstrated that thanks to the versatility of femtosecond laser machining, it is possible to include strain sensors in fused silica compliant mechanisms during their manufacturing [7], [8]. In this work, the elastic range of fused silica for micro-scale compliant mechanisms is studied. Estimations of the bending strength are presented for different flexure specimens. The results are compared to the previously reported value of 2.7 GPa [9]. Then, the damping characteristics of the fused silica flexure specimens are studied for their potential use as resonators.

Fused silica, with its high-temperature stability and low-damping behaviour, is also a well-suited material for precision sensors. The operating range of a sensor based on an oscillator can be limited by thermal noise in the low-frequency domain [10]. Using low-damping materials, this noise is mainly dominated by gaseous thermal noise. Nevertheless, at low frequency and in a low vacuum environment, there is a dissipation occurring inside the material, called thermoelastic damping (TED). Each energy dissipation phenomenon can be included in one term called the quality factor or 'sharpness of resonance': $\frac{1}{Q} = \sum_i \frac{1}{Q_i}$. The smallest Q_i dominates. Fused silica's high-quality factor can differ according to its manufacturing method [11]. Two different experiments are built to extract this characteristic.

The flexure specimen geometries are presented in this work in the first section. Then, the bending strength experiment is described and the results are listed for two different types of flexure elements. In the next section, the quality factor model and experiment are shown for two different scales of resonators based on micro-scale fused silica flexure hinges. Finally, the results are discussed and further approaches are proposed.

II. FLEXURE SPECIMENS

Flexure elements are compliant joints for monolithic mechanisms. Their degrees of freedom are defined by their geometry. A structure can be considered as a flexure element when its thickness is at least ten times smaller than its other dimensions. Then, as this joint is monolithic, it acts like a spring in its degrees of freedom. Therefore, the bending range of such a joint is limited by the bending strength of the material. As fused silica is a brittle material, its bending strength is limited by its surface quality. It depends on the probability of cracks in the structure. So, it explains why the typical bending strength of fused silica is about 50 MPa on the datasheets but can be considered above 1 GPa for micro-scale structures. The two structures tested in this work are described in Fig. 1. The circular notch (Fig. 1 a) is a 3 DoF joint with a stable rotation centre but a limited bending range due to stress concentration. (Fig. 1 b) The free cross-spring hinge is a 1 DoF joint which can have the low stiffness of a leaf spring [12]. The parallel leaf spring joint (Fig. 1 c) is a 2 DoF joint used as the hinge of the pendulum for the vacuum experiment in Section IV B.

[1]Department of Aerospace and Mechanical Engineering, Université de Liège, 4000 Liège, Belgium loic.amez-droz@doct.uliege.be

[2]Transfers, Interfaces & Processes Department, Université libre de Bruxelles, 1050 Brussels, Belgium pierre.lambert@ulb.be

[3]Electromagnetism and Telecommunication Department, UMONS, 7000 Mons, Belgium

[4]BEAMS Department, Université libre de Bruxelles, 1050 Brussels, Belgium

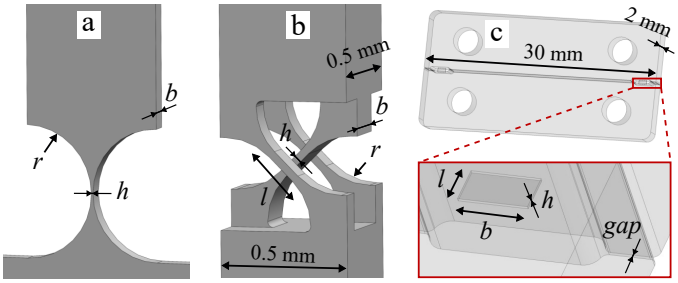

Fig. 1. The flexure specimens. **a** The circular notch of width $b = 500$ µm, with its radius $r = 2$ mm and its central thickness h between 25 µm and 55 µm. **b** The free cross-spring inspired from [12] of total beam width of $2b = 400$ µm, beam length $l = 300$ µm, beam thickness h between 8 µm and 37 µm and with a stress relaxation radius at the extremities of the beam $r = 260$ µm. **c** The parallel leaf-spring hinge joint is designed to hang a pendulum oscillating proof mass. Each leaf spring beam has a width $b = 1$ mm, a length $l = 500$ µm and a thickness $h = 50$ µm. These beams are located in the central thickness of the 2 mm thick monolithic part. A 50 µm gap is etched along the width of this joint to limit the rotation range of the joint.

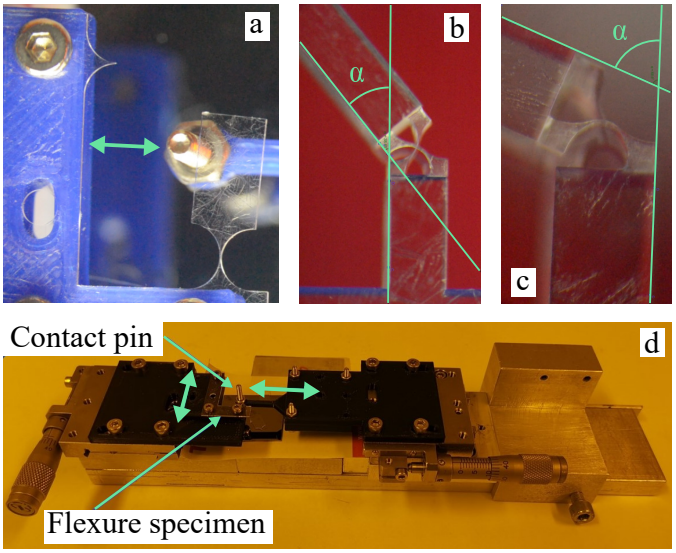

Fig. 2. The flexure specimens. **a** The circular notch of width $b = 500$ µm, with its radius $r = 2$ mm and its central thickness h between 25 µm and 55 µm. **b** The free cross-spring inspired from [12] of total beam width of $2b = 400$ µm, beam length $l = 300$ µm, beam thickness h between 8 µm and 37 µm and with a stress relaxation radius at the extremities of the beam $r = 260$ µm.

III. Bending Strength Estimation

To estimate the bending strength, the flexure specimens are fixed on a 2 DoF translation platform (Fig. 2 d). A rigid pin (a screw or a resistor leg) can push at the free extremity of the rigid body attached to the flexure specimen. A camera placed on top is recording the bending. The specimen is bent until it breaks. Then, the image of the camera just before the rupture of the specimen is extracted. The maximum bending angle can be measured on this image (Fig. 3). The error of this method is less than 1° keeping the stress estimation error to the range ±100 MPa for the thickest specimens. The surface of each of the specimen is checked under the microscope. The surface quality of the specimens is regular thanks to the repeatability of the machining process. However, it happens that specimens have defects such as small notches as shown in [13]. These specimens are then discarded from the test samples. Also, some cracks may appear caused by the manipulation although they are handled carefully.

A. Circular Notch Hinge Bending

From the stiffness of the circular notch and the measured maximum bending angle α_{max}, the maximum bending stress in the specimen can be expressed as [14]:

$$\sigma_{max} = \frac{4E\alpha_{max}\sqrt{h}}{3\pi\sqrt{r}} \tag{1}$$

with E, Young's modulus of fused silica (72 GPa), h, the central thickness of the circular notch and r, the central radius of the circular notch.

B. Triple Beam Cross-Hinge Bending

The free cross-spring hinge has three beams. Due to the manufacturing technique etching aspect ratio, the thickness of the beams varies. A compensation in the design has not been performed. So, the middle beam is thicker and breaks before the other ones. To perform the estimation on a simplified model, the bending angle α_{max} before the last beam brakes is considered. The maximal stress located at the surfaces of the beam can be expressed as:

$$\sigma_{max} = \frac{E\alpha_{max}h}{2l} \tag{2}$$

with h, the thickness of the beams of the cross-hinge and l, their length.

C. Results

The results of the bending experiments are reported in Fig. 3. The estimated maximal bending stress varies from 1.3 GPa to 2.7 GPa for the free cross-hinge specimens and from 1.1 GPa to 2.3 GPa for the circular notch specimens. This experiment consolidates the results obtained in [9]. It also shows that this limit is not dependent on the thickness of the specimen in the studied range (8 µm to 55 µm). The bending strength of fused silica can then be considered as 1 GPa for the design of compliant mechanisms in this thickness range.

IV. Quality Factor Estimation

Fused silica being a low-damping material, it is necessary to analyze the oscillation energy dissipation under vacuum. At ambient pressure, the dissipation is governed by the gaseous damping. To model the dissipation, there are two regimes to consider: at high pressure, the gas acts in a viscous regime. At lower pressure, the air is rarefied. The air molecules are less likely to hit each other. Only the collision between the oscillator and the molecules can be considered. The quality factor can be expressed as [15]:

$$Q_{molecular} = \frac{\rho_b t\omega_0}{4}\sqrt{\frac{\pi}{2}}\sqrt{\frac{RT}{M_{air}}}\frac{1}{p} \tag{3}$$

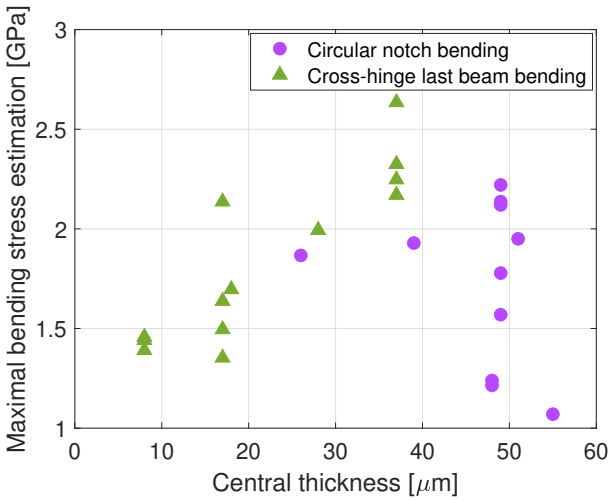

Fig. 3. The maximal bending stress of the element is estimated from their maximum bending angle before rupture.

with ρ_b, the density of the material, t, the thickness of the pendulum, ω_0, its natural resonance frequency, R, the gas constant, M_{air}, the molecular mass of the gas and p, the gas pressure. If the oscillator is close to walls though, another approach has to be considered [16]. For the viscous regime, the quality factor can be described using fluid mechanics as [17] where the oscillator can be considered as a string of spheres, with the diameter equal to the width of the oscillator:

$$Q_{viscous} = \frac{2\rho_b t w^2 \omega_0}{6\pi\mu w + \frac{3}{2}\pi w^2 \sqrt{2\mu \frac{M_{air}}{RT}\omega_0 p}} \tag{4}$$

with w, the characteristic length of the oscillator (for example, its length) and μ, the dynamic viscosity of the gas. The limit between the two regimes can be separated using the Knusden number [18]: $Kn = \frac{\lambda}{w}$, with λ, the mean free path of gas molecules and w, the width of the gas layer in motion. The free molecule regime is considered when $Kn > 10$. The viscous regime is considered when $Kn < 0.1$. In between, there is a transition regime where both phenomena have influence. Other than the gas damping, energy dissipation can occur through the clamping. Vibration waves are propagating through the clamping and are damped in their way before coming back. It means that an amount of the vibrational energy is dissipated through the clamp. The quality factor can be expressed as the clamped-free model in [19]:

$$Q_c = \gamma_0 \frac{L}{t} \tag{5}$$

with γ_0, a vibration mode material dependant constant, L, the length of the oscillator and t, the thickness of its flexure hinge joint. This phenomenon is not reported in this work as it occurs multiple orders of magnitude above the other quality factor models. The quality factor dependent on the material describes its thermoelastic damping (TED). It describes the heat flow dissipation due to internal friction inside the material. It can be expressed as [20]:

$$Q_{TED}^{-1} = \frac{E\alpha_T^2 T}{C_p \rho_b}\left[\frac{6}{\xi^2} - \frac{6}{\xi^3}\frac{sinh(\xi)+sin(\xi)}{cosh(\xi)+cos(\xi)}\right] \tag{6}$$

$$\xi = w\sqrt{\frac{\rho_b C_p \omega_0}{2k}} \tag{7}$$

with α_T, the coefficient of thermal expansion, C_p, the specific heat, w, the width of the flexure hinge joint and k, the thermal conductivity.

A. Ring-Down Experiment - Cross-Hinge

The quality factor is estimated through ring-down experiments. The test bench is represented in Fig. 4. The oscillators composed of a free cross-hinge specimen as its flexure joint are placed inside a small vacuum chamber. A rigid pin located on a 3 DoF translational platform inside the vacuum tank that can be controlled manually from outside is used to bend the oscillator and release it. A glass window is located on top of the tank (in the centre of Fig. 4). A camera is placed on top of this window to record the oscillation. The amplitude of the oscillation is then obtained by image recognition of the trace of the oscillator as in Fig. 4 b. The oscillation damping can be quantified by taking an

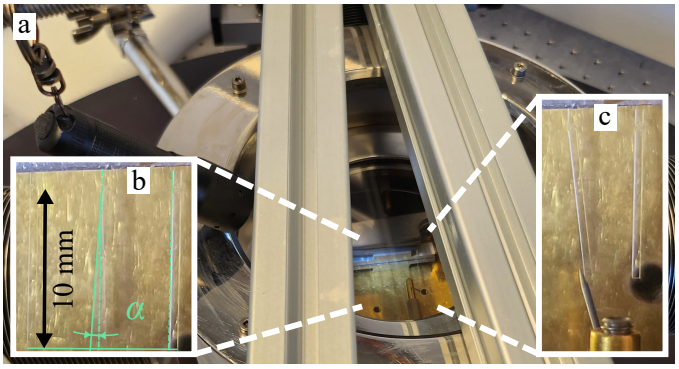

Fig. 4. The test bench to perform the ring-down experiments on the cross-hinge-based oscillators. **a** The vacuum tank with a transparent window at the top, a flashlight on the side to highlight the sides of the glass structure and two Aluminum profiles used as a mount for the camera. **b** The image seen by the camera which is used to extract the bending amplitude of the resonators of length $L = 10$ mm. **c** The translational pin used to apply the starting amplitude to the resonators which are controlled manually from outside the vacuum chamber.

exponential fit of the envelope of the oscillation amplitude in the time domain. The amplitude is described as $A = A_0 e^{-\alpha t}$, with t, the time, A_0, the amplitude at $t = 0$ and α, the attenuation factor. The quality factor is then estimated as:

$$Q = \frac{\omega_0}{2\alpha} \tag{8}$$

with ω_0, the natural resonance frequency of the cross-hinge and α, the attenuation factor of the oscillation extracted from the ring-down experiment as detailed in Fig. 5.

$$\omega_0 = \sqrt{\frac{K_{\theta M}}{I}} \tag{9}$$

with $K_{\theta M} = \frac{Ebh^3}{6l}$, the rotational stiffness of the beams of the cross-hinge and I, the inertia of the oscillator, which can be described as a thin beam attached to the cross-hinge:

$$I = \frac{mL^2}{12} + mr_{CoG}^2 \tag{10}$$

with m, the mass of the 500 µm side squared oscillator of length L and r_{CoG}, the distance between its Centre of Gravity and the centre of the cross-hinge. The obtained resonance frequency $f_0 = \frac{w_0}{2\pi}$ has been verified experimentally. A vibrometer has been placed instead of the camera. The resonance frequency has been then extracted by recognition of the resonator cyclic pattern period.

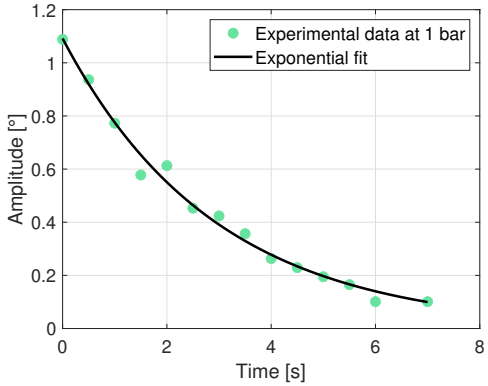

Fig. 5. The bending amplitude of the resonators. Each green point in the graph corresponds to the maximal amplitude of the trace of the beam extracted from a picture as in Fig. 4 b.

B. Ring-Down Experiment - Pendulum

Ring-down experiments are also performed on a larger pendulum. An Aluminium proof mass is suspended using the parallel leaf spring fused silica flexure joint described in Fig. 1. This pendulum is placed inside a larger vacuum tank (Fig. 6). There is a transparent window located on top of the vacuum tank. A vibrometer OFV 500 from Polytec is used to record the oscillation of the pendulum. The laser head is placed outside from the tank on top of the window facing a mirror. The mirror reflecting the laser is placed at 45° from the laser head and at 45° from the pendulum (Fig. 6 c). The quality factor can be extracted by performing an exponential fit on the envelope of the amplitude signal recorded with the vibrometer.

$$Q = \frac{\omega_0}{2\alpha} \tag{11}$$

with ω_0, the natural resonance frequency of the pendulum extracted from the ring-down vibrometer oscillation amplitude signal and α, the attenuation factor of the oscillation extracted from the ring-down experiment.

C. Results

The quality factor extracted from both experiments is reported in Fig. 7. Both experiments are compared to the study of Bianco et al. [18]. They studied the quality factor of a silicon cantilever beam of width $b = 100$ µm, length

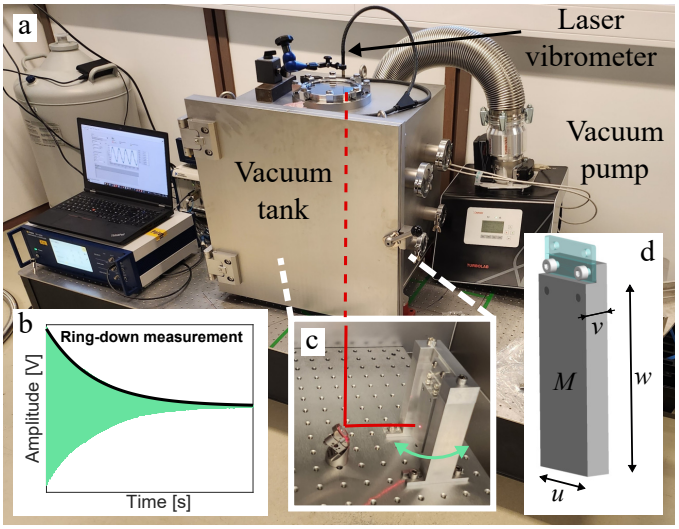

Fig. 6. The test bench to perform the ring-down experiments on the parallel leaf spring-based pendulum. **a** The test bench is composed of a vacuum tank, a vibrometer and the data acquisition system (DAQ). **b** The amplitude time measurement of the pendulum recorded with the vibrometer. **c** The pendulum is located inside the vacuum tank facing the 45° mirror. **d** The pendulum geometry of width $u = 30$ mm, length $w = 82$ mm, thickness $v = 10$ mm and of mass $M = \rho_{Al} uvw$.

$l = 800$ µm and thickness $h = 5$ µm. The quality factor data of the cross-hinge-based resonators compare with the model. Unfortunately, it was not possible to decrease the pressure in the small tank below 2×10^{-3} mbar. So, this experiment is not sufficient to quantify the thermoelastic noise described by the slope tending to saturation at low pressure. The maximal Q-factor obtained at $p = 2 \times 10^{-3}$ mbar is $Q = 1.85 \times 10^5$. However, these results are promising. This maximum value is higher than the one reported in [18] about the silicon cantilever ranging in the same dimension scale. Regarding the leaf spring-based pendulum experiment, there is an unexpected saturation at $Q = 2.5 \times 10^4$. The dissipation source is probably not explained by clamping dissipation as it faces almost the same conditions as the other experiment. A hypothesis is that the load applied to the small flexure joint induces stress that may influence the internal friction in the leaf springs. However, the contrary is reported explaining that applying tensile stress leads to a decrease in the thermoelastic damping [21]–[23]. Then, other approaches need to be investigated. The asymmetry of the manufactured part or its surface quality under tensile stress may lead to dissipation. Or friction at the fused silica-aluminium boundary may occur.

V. CONCLUSIONS

This work consolidates the design rule that 1 GPa bending strength can be considered for fused silica micro-scale structures. Nevertheless, as the effect of surface quality has not been quantified in this work, this limit is valid for parts manufactured in the same conditions. Continuing with bending strength, a study reported that annealing the fused silica part machined through femtosecond laser-assisted wet

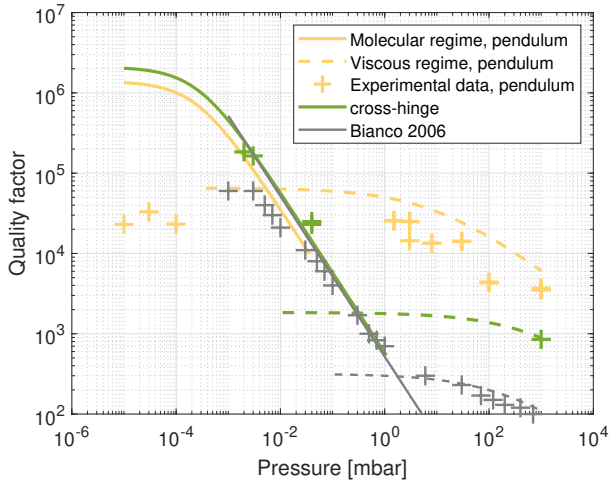

Fig. 7. The estimations of the quality factor obtained through the ring-down experiments at different pressures. In green, the model and data correspond to the cross-hinge-based resonators. In yellow, are the model and data corresponding to the parallel leaf springs-based pendulum. In grey, are the model and data reconstructed from the work of Bianco et al. [18].

etching increases their compressive strength [24]. Our experimental method can be used to investigate if annealing has a significant impact on bending strength. To assess the dynamic properties of fused silica, the damping characteristics have been investigated for two different configurations. The quality factor of the free cross-hinge-based fully monolithic fused silica resonators is not limited by thermoelastic damping at pressures above 2×10^{-3} mbar. An improvement on the setup is necessary to perform ring-down experiments at lower pressures. The quality factor of the parallel leaf spring-based loaded pendulum saturates at $Q = 2.5 \times 10^4$ below 1 mbar. A deeper study is required to explain this dissipation. An investigation of whether annealing the fused silica flexure specimens has an influence or not on their damping characteristics is planned.

ACKNOWLEDGMENT

The authors gratefully acknowledge the "Fonds de la Recherche Scientifique", Research project grant INFuSE (grant agreement number FNRS PDR T.0049.20 and GEQ FEMTOPrint U.G025.19F), for funding this research.

REFERENCES

[1] Y. Bellouard, A. Champion, B. Lenssen, M. Matteucci, A. Schaap, M. Beresna, C. Corbari, M. Gecevičius, P. Kazansky, and O. Chappuis, "The femtoprint project," *Journal of Laser Micro/Nanoengineering*, vol. 7, no. 1, pp. 1–10, 2012.

[2] Y. Bellouard, A. A. Said, and P. Bado, "Integrating optics and micromechanics in a single substrate: a step toward monolithic integration in fused silica," *Optics Express*, vol. 13, no. 17, pp. 6635–6644, 2005.

[3] B. Lenssen and Y. Bellouard, "Optically transparent glass microactuator fabricated by femtosecond laser exposure and chemical etching," *Applied Physics Letters*, vol. 101, no. 10, p. 103503, 2012.

[4] S. I. Nazir and Y. Bellouard, "Contactless optical packaging concept for laser to fiber coupling," *IEEE Transactions on Components, Packaging and Manufacturing Technology*, vol. 11, no. 6, pp. 1035–1043, 2021.

[5] M. Zanaty, T. Fussinger, A. Rogg, A. Lovera, D. Lambelet, I. Vardi, T. J. Wolfensberger, C. Baur, and S. Henein, "Programmable multistable mechanisms for safe surgical puncturing," *Journal of Medical Devices*, vol. 13, no. 2, 2019.

[6] L. Tissot-Daguette, C. Baur, A. Bertholds, P. Llosas, and S. Henein, "Design and modelling of a compliant constant-force surgical tool for objective assessment of ossicular chain mobility," in *2021 21st International Conference on Solid-State Sensors, Actuators and Microsystems (Transducers)*. IEEE, 2021, Conference Proceedings, pp. 1299–1302.

[7] M. Tunon de Lara, L. Amez-Droz, K. Chah, P. Lambert, C. Collette, and C. Caucheteur, "Femtosecond pulse laser-engineered glass flexible structures instrumented with an in-built bragg grating sensor," *Optics Express*, vol. 31, no. 18, pp. 29 730–29 743, 2023.

[8] L. Amez-Droz, M. Tunon de Lara, C. Collette, C. Caucheteur, and P. Lambert, "Instrumented flexible glass structure: A bragg grating inscribed with femtosecond laser used as a bending sensor," *Sensors*, vol. 23, no. 19, p. 8018, 2023.

[9] Y. Bellouard, "On the bending strength of fused silica flexures fabricated by ultrafast lasers," *Optical Materials Express*, vol. 1, no. 5, pp. 816–831, 2011.

[10] P. R. Saulson, "Thermal noise in mechanical experiments," *Physical Review D*, vol. 42, no. 8, p. 2437, 1990.

[11] K. Numata, S. Otsuka, M. Ando, and K. Tsubono, "Intrinsic losses in various kinds of fused silica," *Classical and Quantum Gravity*, vol. 19, no. 7, p. 1697, 2002.

[12] V. Tielen and Y. Bellouard, "Three-dimensional glass monolithic micro-flexure fabricated by femtosecond laser exposure and chemical etching," *Micromachines*, vol. 5, no. 3, pp. 697–710, 2014.

[13] C.-E. Athanasiou, M.-O. Hongler, and Y. Bellouard, "Unraveling brittle-fracture statistics from intermittent patterns formed during femtosecond laser exposure," *Physical Review Applied*, vol. 8, no. 5, p. 054013, 2017.

[14] S. Henein, "Conception des structures articulées à guidages flexibles de haute précision," EPFL," Report, 2000.

[15] R. Christian, "The theory of oscillating-vane vacuum gauges," *Vacuum*, vol. 16, no. 4, pp. 175–178, 1966.

[16] M. Bao, H. Yang, H. Yin, and Y. Sun, "Energy transfer model for squeeze-film air damping in low vacuum," *Journal of Micromechanics and Microengineering*, vol. 12, no. 3, p. 341, 2002.

[17] H. Hosaka, K. Itao, and S. Kuroda, "Damping characteristics of beam-shaped micro-oscillators," *Sensors and Actuators A: Physical*, vol. 49, no. 1-2, pp. 87–95, 1995.

[18] S. Bianco, M. Cocuzza, S. Ferrero, E. Giuri, G. Piacenza, C. Pirri, A. Ricci, L. Scaltrito, D. Bich, and A. Merialdo, "Silicon resonant microcantilevers for absolute pressure measurement," *Journal of Vacuum Science & Technology B: Microelectronics and Nanometer Structures Processing, Measurement, and Phenomena*, vol. 24, no. 4, pp. 1803–1809, 2006.

[19] Z. Hao, A. Erbil, and F. Ayazi, "An analytical model for support loss in micromachined beam resonators with in-plane flexural vibrations," *Sensors and Actuators A: Physical*, vol. 109, no. 1-2, pp. 156–164, 2003.

[20] R. Lifshitz and M. L. Roukes, "Thermoelastic damping in micro-and nanomechanical systems," *Physical review B*, vol. 61, no. 8, p. 5600, 2000.

[21] Y. Huang and P. R. Saulson, "Dissipation mechanisms in pendulums and their implications for gravitational wave interferometers," *Review of scientific instruments*, vol. 69, no. 2, pp. 544–553, 1998.

[22] S. Kumar and M. Haque, "Reduction of thermo-elastic damping with a secondary elastic field," *Journal of sound and vibration*, vol. 318, no. 3, pp. 423–427, 2008.

[23] A. S. Vahdat and G. Rezazadeh, "Effects of axial and residual stresses on thermoelastic damping in capacitive micro-beam resonators," *Journal of the Franklin Institute*, vol. 348, no. 4, pp. 622–639, 2011.

[24] R. N. Widmer, D. Bischof, J. Jurczyk, M. Michler, J. Schwiedrzik, and J. Michler, "Smooth or not: Robust fused silica micro-components by femtosecond-laser-assisted etching," *Materials & Design*, vol. 204, p. 109670, 2021.